Knocking on surfaces : interactions of hyperthermal particles with metal surfaces

Ueta, H.

Chapter 4

CO Blocking of D_2 Dissociative Adsorption on Ru(0001)

The influence of pre-adsorbed CO on the dissociative adsorption of D_2 on Ru(0001) is studied by molecular-beam techniques. We determine the initial dissociation probability of D_2 as a function of its kinetic energy for various CO pre-coverages between 0.00 and 0.67 monolayers (ML) at a surface temperature of 180 K. The results indicate that CO blocks D_2 dissociation and perturbs the local surface reactivity up to the nearest-neighbour Ru atoms. Non-activated sticking and dissociation become less important with increasing CO coverage, and vanish at $\theta_{CO} \approx 0.33$ ML. In addition, at high D_2 kinetic energy (>0.35 eV) the site-blocking capability of CO decreases rapidly. These observations are attributed to a CO-induced activation barrier for D_2 dissociation in the vicinity of CO molecules.

4.1 Introduction

In most heterogeneously catalysed reactions at least two reactants interact with a solid surface simultaneously. For this reason, interactions and chemical reactions between molecules and atoms co-adsorbed on well-defined metal surfaces have received considerable attention. An overview of the work in this area can be found in a variety of reviews [1-4]. It is important to unravel the influence of adsorbates on the dynamics of adsorption and dissociation of other species from the gas phase. Studies in this area have mainly focused on the poisoning or promotional activity of pre-adsorbed electronegative and electropositive atoms toward activated dissociation of different reactants [5]. These studies are of particular interest when the activation barrier to adsorption of a reactant may be rate-determining for the overall kinetics.

The interaction between CO and H_2 on ruthenium is a particularly interesting system because of its relevance to Fischer–Tropsch synthesis and the methanation reaction [6-9]. Individually, CO and H_2 adsorption on Ru (0001) has already been studied in detail. CO adsorption is non-activated and non-dissociative [10-13]. Adsorption takes place by donation of CO 5s electrons to the substrate and back-donation from the metal into the unoccupied 2p* orbital of CO [14, 15]. The molecule attaches to the surface through the C end at all coverages [16-18], with the on-top position preferred up to a CO coverage θ_{CO} of 1/3 monolayers (ML) [19-22]. For surface temperatures T_S below 150 K and $\theta_{CO} \leq 1/3$ ML, a lattice gas is in equilibrium with $(\sqrt{3} \times \sqrt{3})$R30° islands [23]. For $\theta_{CO} > 1/3$ ML, several complex structures, dependent both on θ_{CO} and T_S, have been observed. At $\theta_{CO}=1/2$ ML, a full $(2\sqrt{3} \times \sqrt{3})$R30° structure is formed [11]. A $(2\sqrt{3} \times 2\sqrt{3})$R30° structure at $\theta_{CO}=7/12$ ML has been reported [18]. Finally, at saturation ($\theta_{CO} \approx 2/3$ ML), a $(5\sqrt{3} \times 5\sqrt{3})$R30° structure was observed by means of He atom scattering (HAS) [24, 25].

In contrast to CO, hydrogen is adsorbed dissociatively on Ru(0001). Experimental studies found non-activated adsorption in addition to a direct, activated mechanism occurring on a distribution of barriers [26, 27]. Our studies of H_2 and D_2 dissociation indicate that there is no isotope effect over a wide kinetic energy range and normal energy (E_n) scaling is observed [27]. The H atoms produced by dissociative adsorption bind preferentially in the fcc threefold-hollow sites [28]. The saturation coverage is unity (relative to Ru surface atoms) [29].

The interaction between CO and H(D) co-adsorbed on Ru(0001) has also been studied. At $T_S=100$ K, no evidence was found for a chemical reaction between H(D) and CO [30]. From shifts in the thermal desorption states of D_2 in temperature programmed desorption (TPD), a repulsive CO–H(D) interaction was found. These early observations were supported by a study on surface diffusion of hydrogen by laser-induced thermal desorption techniques [31], an HAS study [24], a combined infrared absorption spectroscopy and density functional theory (DFT) study [32] and a study combining TPD and thermal-energy He atom scattering (TEAS) [33]. Whereas the bare Ru(0001) surface shows no activation barrier to CO adsorption, DFT

calculations and measurements of sticking probability revealed that the H-passivated surface has an activation barrier for CO adsorption of at least 0.26 eV [12, 13].

The present study follows up on our previous investigation of the dynamics of H_2/D_2 dissociation on bare Ru(0001) [27]. Herein, we probe the dynamics of D_2 dissociation on CO-covered Ru(0001). We use TPD and molecular beam techniques to determine the dissociation probability (S) of D_2 at T_S=180 K as a function of its kinetic energy (E_i) and the CO pre-coverage. Combined with a simple site-blocking model and information from a gas-phase *ab initio* potential, our results give insight into the mechanisms by which CO modifies D_2 dissociation on Ru(0001).

4.2 Experimental

The experiments were performed in a molecular-beam apparatus, details of which have been published previously [27, 34]. Briefly, it consists of a triply differentially pumped molecular beam line connected to an ultrahigh-vacuum (UHV) chamber with an ion sputter gun and a residual gas analyser (RGA). A differentially pumped quadrupole mass spectrometer (QMS) is mounted on a linear drive in line of sight with the molecular beam. This QMS is used to measure the velocity distribution of incident D_2 by time-of-flight techniques, and to measure TPD spectra. The sample is mounted in the centre of the UHV chamber on a rotatable manipulator, which allows the angle of incidence of the molecular beam to be varied with respect to the surface.

The Ru(0001) crystal used for these studies was oriented to within 0.1° of the (0001) face. The surface was cleaned by repeated cycles of Ar^+ sputtering followed by annealing to 1500 K for several minutes and then annealing for several minutes at 1200 K in an oxygen atmosphere (1×10^{-8} mbar O_2). The final cleaning step was Ar^+ sputtering followed by annealing to 1500 K for several minutes. The surface cleanliness was checked by reference to the TPD spectra of CO and NO.

To prepare a CO-covered surface, background dosing of CO was performed at surface temperatures less than 200 K. The dosing of CO on Ru(0001) was calibrated on the basis of the integrated TPD signals. Absolute θ_{CO} values were determined by comparison with the value for CO saturation coverage. The saturation coverage was assumed to be 2/3 ML (relative to Ru surface atoms).

The incident kinetic energy of D_2 was controlled by nozzle-heating (room temperature to 1700 K) and seeding D_2 (purity 99.8%) in H_2 (99.9999 %). Assuming no vibrational relaxation during beam expansion, the population of the Boltzmann vibrational distribution in the ground state (v=0) would be about 93% at the highest nozzle temperature of 1700 K, so that vibrational excitation can be considered to have little or no influence on D_2 dissociation in our experiments. However, due to poor rotational cooling of $D_2(H_2)$ during supersonic expansion at high nozzle temperatures [35, 36], our high-energy beams have broad translational- and rotational-energy distributions, in particular at the highest temperature [27].

The D_2 sticking probability was measured by using the adsorption reflection technique of *King and Wells* [37, 38]. The partial D_2 pressure was monitored by an

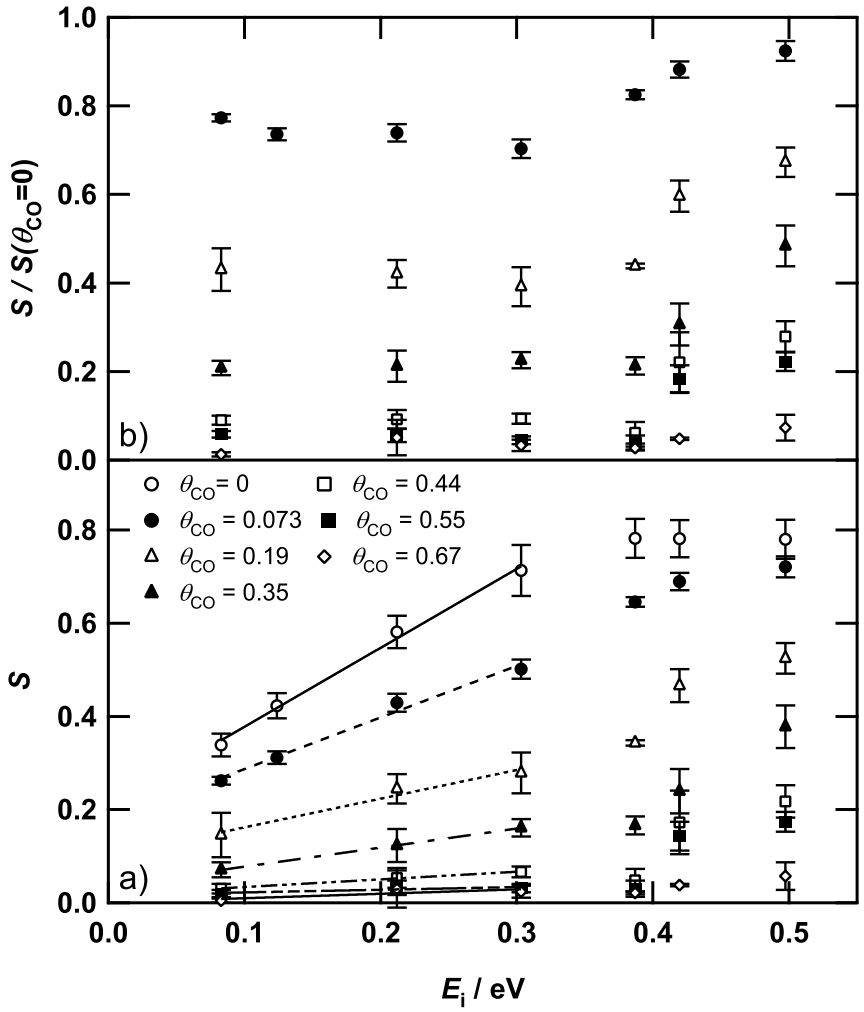

Figure 4. 1 (a) Dissociation probability S of D_2 on CO-covered Ru(0001) (θ_{CO}=0–2/3 ML) at normal incident angle as a function of D_2 kinetic energy for T_S=180 K. The lines are obtained by linear fitting of data points for E_i<0.3 eV for each S curve in order to extrapolate the value of S to zero kinetic energy. (b) The values of S for each θ_{CO} after normalisation by the corresponding S for bare Ru(0001) as a function of D_2 kinetic energy.

RGA. From experiments confirming dissociative chemisorption of H_2/D_2 on Ru(0001), it is well-established that the sticking probability is a direct measure of the dissociation probability. Hence, the term "dissociation probability" is used throughout this paper. In order to measure the initial dissociation probability, the D_2 beam flux was strongly reduced by using a 2% duty-cycle chopper. The D_2 beam impinges on the surface at normal incidence. During exposure to D_2 the surface temperature was held constant at 180 K.

4.3 Results

The adsorption behaviour of CO on the Ru(0001) surface is dependent on T_S and θ_{CO}. The phase diagram of CO adsorbed on Ru(0001) has been reported on the basis of

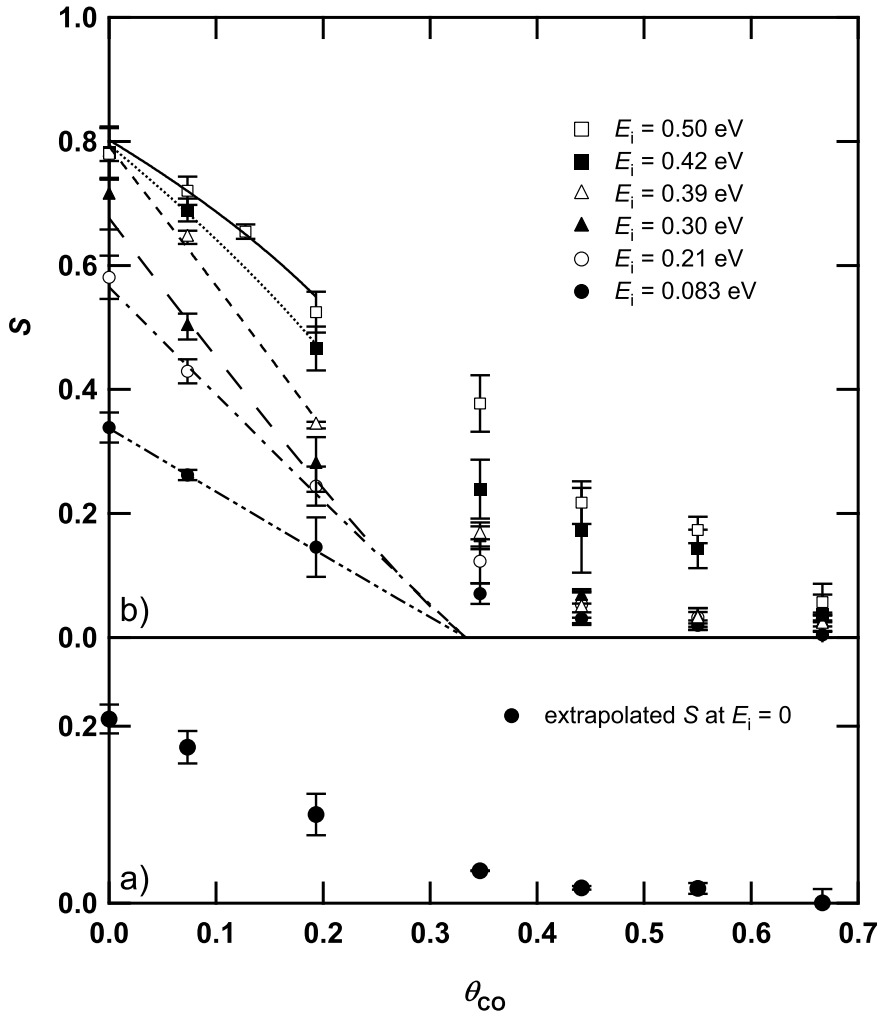

Figure 4. 2 (a) The values of S after extrapolation to zero kinetic energy, as a function of θ_{CO}. These values are obtained from linear fits to the data shown in figure 4.1(a). (b) Dependence of S of D_2 on θ_{CO} for CO-covered Ru(0001) at six different initial kinetic energies. The lines are fits to the data by using equation (4.1).

low-energy electron diffraction and theoretical studies [23, 39-41]. Under our experimental conditions (T_S=180 K), CO molecules are randomly adsorbed on the surface up to $\theta_{CO}\approx$0.2 ML (lattice gas). Beyond this coverage, the CO overlayer shows several complex phases, such as $(\sqrt{3}\times\sqrt{3})$R30° and $(2\sqrt{3}\times 2\sqrt{3})$R30°, which depend on θ_{CO}.

The variation of S as a function of D_2 kinetic energy is shown in figure 4.1(a) for several CO pre-coverages. In general, S increases monotonically with increasing D_2 kinetic energy up to a value of about 0.3 eV. The increase in dissociation probability with increasing D_2 kinetic energy suggests that D_2 dissociation on the CO-covered Ru(0001) is mainly an activated process. The relative and absolute changes in S as a function of kinetic energy are the largest for the bare Ru surface. With increasing θ_{CO}, the increase in S with kinetic energy is smaller. For saturation coverage (θ_{CO}=2/3 ML) it is difficult to say within experimental error whether S is constant or very gradually changes with the D_2 kinetic energy.

For E_i greater than about 0.3 eV, there is a θ_{CO}-dependent change in the behaviour of S as a function of E_i. For θ_{CO}<0.2 ML, S appears to reach a plateau, and the maximum value of S decreases with increasing θ_{CO}. In contrast, for θ_{CO}>0.2 ML the increase in S as a function of E_i is greater above 0.3 eV than below that energy. The values of S after normalisation by S for the bare Ru surface are shown as a function of E_i in figure 4.1(b). From this figure, the magnitude of the relative increase in S for E_i>0.3 eV is evident. This suggests that, particularly for high θ_{CO}, values of E_i greater than 0.3 eV open a new dissociation path that is inaccessible, at those coverages, to D_2 with lower kinetic energies.

Studies of H_2/D_2 dissociation on the bare Ru(0001) surface indicate not only an activated process, but also a non-activated process [26, 27]. From figure 4.1(a), a value for S at zero kinetic energy can be extrapolated from the linear range of each dissociation probability curve, if we assume a linear relationship between E_i and S. These values are plotted in figure 4.2(a) as a function of CO coverage. The value of S at zero kinetic energy decreases linearly with increasing θ_{CO}. Figure 4.2(a) indeed implies the presence of a non-barrier (or low-barrier) site for D_2 dissociation at the bare surface that is blocked by CO adsorption. The data of figure 4.1(a) are re-plotted in figure 4.2(b), showing S as a function of CO coverage for different kinetic energies of D_2. Clearly, S decreases with increasing θ_{CO} at all energies. Hence, CO acts as a poison for D_2 dissociation on the Ru(0001) surface. In the discussion, we examine the details of this poisoning effect as a function of θ_{CO}. Our main interest is in the initial dissociation probability of D_2 before appreciable concentrations of D atoms have accumulated on the surface. However, we also estimated the total amount of D_2 that can be adsorbed at each CO coverage from our data. These estimates are in excellent agreement with the measurements of Peebles *et al*. [30].

4.4 Discussion

First we consider what, if any, influence incident D_2 molecules have on the adsorbed CO. Kinetic energy transfer from D_2 to CO may result in CO translational motion parallel to the surface. Conservation of momentum parallel to the surface implies that the kinetic energy imparted to CO cannot exceed $(m_{CO}m_{D_2}/M^2)E_i$=0.109E_i, where M=m_{CO}+m_{D_2} (e.g. see ref. [42]). At the highest kinetic energy used in our experiment, CO could acquire at most 0.054 eV parallel to the surface. Although a theoretical study has claimed barrier-free diffusion [43], in an experimental study Deckert *et al.* found barriers of E_{diff}≈0.48 eV for θ_{CO}=0.27 ML and E_{diff}≈0.27 eV for θ_{CO}=0.58 ML [44]. Our maximum values for energy transfer into lateral motion of CO are substantially lower. Therefore, we do not expect significant energy-transfer-induced translational diffusion of CO. Note, however, that since the frustrated translation mode of CO parallel to the surface is about 5.9 meV for an isolated molecule [19, 21, 24, 45], this mode could be excited by D_2 collision under the current experimental conditions.

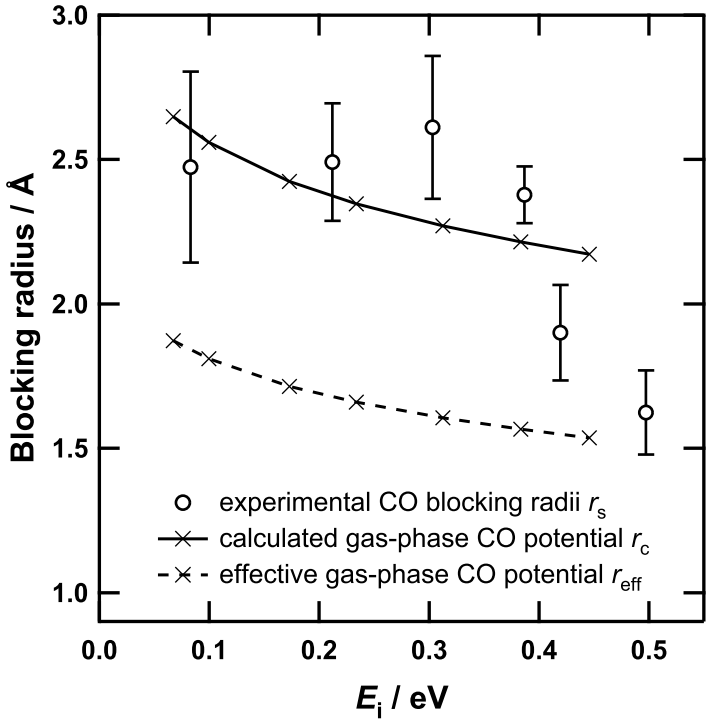

Figure 4. 3 Plot of the radii of Σ_{CO} as a function of D_2 kinetic energy. These values are obtained from fitting equation (4.1) to the data shown in figure 4.2 for the appropriate coverage region (θ_{CO}<0.2 ML). The error bars represent estimated standard deviations in the blocking radii. The solid line with crosses gives the maximum radius r_c of the gas phase H_2—CO interaction potential contour at each energy. The dashed line with crosses gives which in the hard-hemisphere model is the radius below which D_2 molecules would be scattered away from the surface.

Even if the diffusion of CO is barrierless, the post-collision relative speeds of the two molecules imply that a stationary CO picture should be adequate. The postcollision speed of CO can be no more than (m_{D_2}/m_{CO}), or 1/7 that of D_2. In the time that it would take a freely moving CO molecule to move from an on-top site to an adjacent hollow site (ca. 1.56 Å), the corresponding D_2 would move nearly 11 Å, well outside the range of interaction. Consequently, the influence of CO on D_2 dissociation can be discussed without the requirement to consider molecular diffusion.

Since CO shows differing adsorption structures in various coverage ranges, we simplify our analysis by initially focusing only on the lattice-gas region (θ_{CO}<0.2 ML). In this region, CO is randomly adsorbed on the on-top positions of Ru atoms, with CO adsorption on the nearest-neighbour sites of an already occupied site forbidden due to the strong repulsive interactions between the nearest-neighbour CO molecules [17, 18, 45]. If this adsorption behaviour continues in an uninterrupted fashion, the maximum coverage that will arise is θ_{CO}=1/3 ML [17, 20, 46]. In the lattice-gas region, the variation of dissociation probability as a function of CO coverage can be represented by equation (4.1)

$$S(E_i,\theta_{CO}) = S(E_i,0)\left(1-3\theta_{CO}\right)^{n_S\Sigma_{CO}/3} \qquad (4.1)$$

where $S(E_i,0)$ is the dissociation probability for the bare surface, n_S the density of Ru atoms in the (0001) surface, and Σ_{CO} the effective cross section for blocking of dissociative adsorption of D_2 by an adsorbed CO molecule. This equation was obtained by analogy to the TEAS lattice-gas model [47]. The Σ_{CO} in TEAS is due to the removal by CO of specular reflection of He from the flat metal surface. In TEAS, Σ_{CO} is determined by the long-range attractive part of the He—CO potential [47, 48]. The model underlying equation (4.1) assumes that CO completely blocks dissociation of D_2 at θ_{CO}=1/3 ML. Although the data in figure 4.2 do not strictly follow that assumption, equation (4.1) is sufficient for evaluating variations in the blocking cross section at $\theta_{CO}\leq$0.2 ML. The cross sections Σ_{CO} extracted from equation (4.1) are equivalent to cross sections from the more fundamental definition of equation (4.2) but allow us to make better use of the data at modest coverages.

$$\Sigma_{CO} = -[1/n_S S(E_i,0)](dS/d\theta_{CO})_{\theta_{CO}\to 0} \qquad (4.2)$$

Figure 4.2(b) shows fits of equation (4.1) to the experimental data for the CO coverage region θ_{CO}<0.2 ML. The fits establish a value for Σ_{CO} for each value of D_2 kinetic energy. Figure 4.3 shows the resulting dependence of the corresponding cross section radius $r_s=(\Sigma_{CO}/\pi)^{1/2}$ on the D_2 kinetic energy. In the regime of low D_2 kinetic energy, r_s is effectively constant within experimental uncertainty. For E_i>0.35 eV, r_s decreases rapidly.

The values of r_s for E_i<0.35 eV are slightly smaller than the circular area defined by a radius corresponding to the Ru–Ru nearest-neighbour distance (2.71 Å). We conclude that the influence of CO adsorption on D_2 dissociation is quite localised.
Our Σ_{CO} is much smaller than that previously obtained for H_2 and He scattering from CO-covered Pt(111) surface by using the TEAS technique [49-51], that is, in the present case scattering from the repulsive wall largely determines the size of the cross section. Of course, under our experimental conditions, D_2 will also be influenced by the D_2—CO attractive potential, but this attractive well is very small (for gas-phase

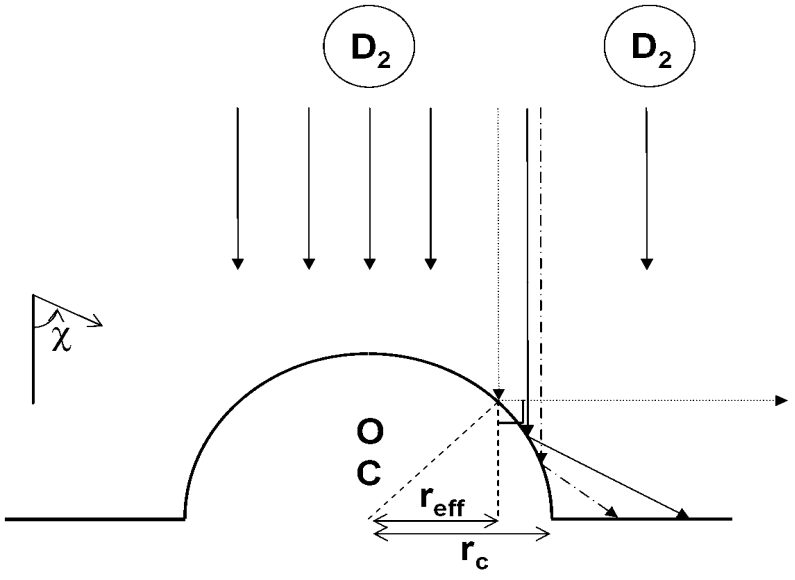

Figure 4. 4 Schematic diagram of the hard-hemisphere collision model. D_2 is treated as a point particle (shown in two positions as circles) and CO is regarded as a hemisphere.

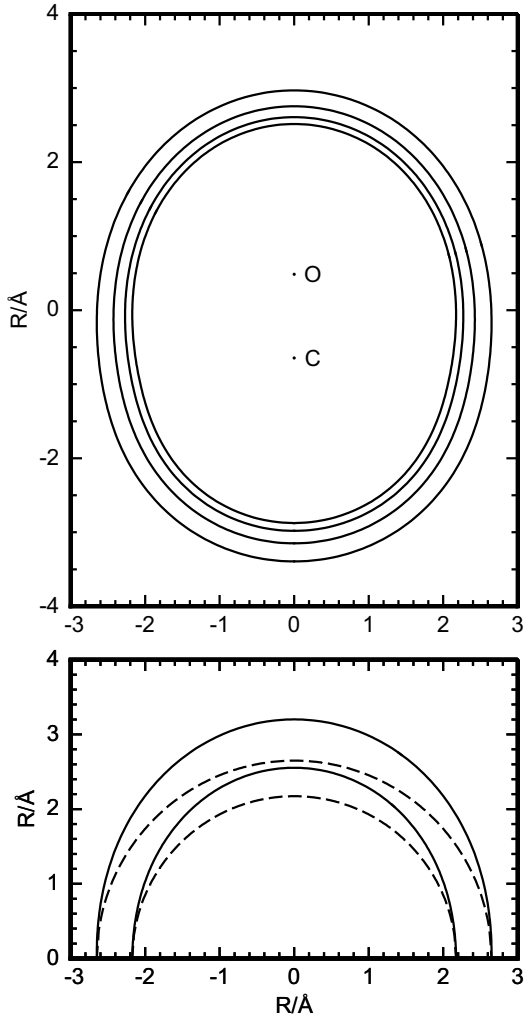

Figure 4. 5 Top: repulsive-wall contours of the H_2-orientation-averaged Jankowski–Szalewicz potential. From outermost to innermost the interaction energies are 0.067, 0.17, 0.31 and 0.45 eV. Bottom: hard-shell interactions as used for modelling of interactions between D_2 and adsorbed CO. Solid lines represent repulsive wall contours of vertically oriented CO, with oxygen end-up, shifted vertically so that the maximum width appears at the horizontal axis. Dashed lines represent the corresponding hard-hemisphere models. The outer pair of curves represents the 0.067 eV contour; the inner pair represents 0.45 eV.

scattering the depth of the D_2—CO attractive well is 5.74 meV [48, 52]) compared to the magnitude of the D_2 kinetic energy that we used. In TEAS the effect of the attractive potential is much larger, because TEAS is sensitive to very small deflections (<1°) of He atoms. In the present case such deflections will not affect the adsorption dynamics in any way.

We now introduce a simple hard-(hemi)sphere collision model to visualise the interaction of D_2 with an isolated CO molecule bound to the Ru(0001) surface [53, 54]. This model is schematically represented in figure 4.4. In the model, D_2 and CO are regarded as a point particle and a hard-hemisphere with relative masses of 4 and

28, respectively. The radius r_c of the hemisphere corresponds to the collision diameter. We determined values of r_c from the *ab initio* H_2—CO potential V_{04} of Jankowski and Szalewicz [55], without attempting to account for changes in CO electronic structure induced by binding to the surface. We averaged the V_{04} potential over the H_2 orientation, and then extracted potential contours on the repulsive wall over the range of centre-of-mass collision energies used in the experiment. At each collision energy, the maximum distance of the potential contour at that energy from the CO internuclear axis was used as r_c. In other words, these values of r_c correspond to the radii of the CO repulsive wall as seen looking along the internuclear axis. Figure 4.5 shows the relation between the accurate CO repulsive wall contours and the corresponding hard-hemisphere models for collision energies near the lowest and highest energies used in our experiments.

In figure 4.3 the solid line with crosses shows the values of r_c we obtained from the H_2—CO potential. They decrease with increasing H_2 kinetic energy, since potential contours higher on the CO repulsive wall are used as the energy increases. If a hard-shell model with these values of r_c is appropriate, and there is no modification of the surface reactivity in the vicinity of the adsorbed CO, then we would expect r_c to be larger than the maximum value of the blocking cross section that could be observed. D_2 molecules that hit the surface beyond r_c would be able to react as they would on the bare surface, and this makes r_c a strict upper bound on the blocking cross section in this model. In addition, some D_2 molecules would hit CO but be redirected toward CO-uncovered surface, as indicated in figure 4.4. These redirected molecules would be expected to have a nonzero dissociation probability corresponding to the θ_{CO}=0 curve from figure 4. 1(a), but with lower "normal energy" E_n'=E' $\cos^2\chi$, where E' is the translational energy of the scattered D_2. Earlier work demonstrated that the H_2/D_2 dissociation probability on the bare Ru surface is exclusively dependent on E_n [27]. Only D_2 molecules with laboratory deflection angles χ greater than 90° would have no chance to react. We would therefore expect the observed blocking radius at any energy to be smaller than r_c.

In the hard-hemisphere model, the critical impact parameter that produces χ=90° is $r_c/\sqrt{2}$, called r_{eff} in figure 4.4. The dashed line with crosses in figure 4.3 denotes r_{eff} values derived from the r_c values. Within the hard-hemisphere, unmodified surface model, this curve represents the minimum value of blocking radius that could be observed. If one uses the realistic hard-shell contours shown in the bottom panel of figure 4.5, rather than the hard-hemisphere approximation, the minimum radii occur at somewhat lower values because of the elongation of the CO potential: about 1.6 Å at the lowest energy shown.

The experimental results shown in figure 4.3 differ in two ways from the expectations outlined for the hard-hemisphere, unmodified-surface model. First, for incident energies less than 0.35 eV, the experimental blocking radii are approximately comparable to or even larger than the upper bounds represented by r_c. Second, the observed blocking radii drop sharply above 0.35 eV. We now consider several possible explanations for these features.

The hard-hemisphere model ignores the attractive and low energy repulsive parts of the potential. It is reasonable to expect that the attractive potential at long range might increase the observed blocking radius by pulling incoming D_2 toward CO, which would reduce its effective impact parameter and increase its scattering angle and translational energy loss. This effect might contribute to the relatively high blocking radius observed at the lowest experimental energies. However, because the depth of the attractive well is less than 10% of our lowest collision energy, the importance of the attractive well must be small, and it should diminish smoothly with increasing collision energy. Certainly it cannot account for the large blocking radii seen at energies near 0.3 and 0.4 eV. Similarly, our replacement of the smooth rise of the potential on the low-energy repulsive wall with a hard barrier at the turning point could produce a modest quantitative shift, but at most could be expected to reduce r_c by one or two tenths of an angstrom. Both the attractive and soft repulsive parts of the potential should become less important as the collision energy increases, so neither can explain the drop in the blocking radius observed at high energies.

One possible explanation for the fall in blocking radius at high energy lies in the shape of the curve of dissociation probability as a function of "normal energy" for the bare surface, shown as open circles in figure 4.1(a). The dissociation probability increases roughly linearly with energy up to just above 0.35 eV, and then remains constant with increasing energy. Therefore, when the initial energy is above the "plateau energy", some collisions with CO will not reduce the dissociation probability at all, because they will reduce the normal energy but to a value still above the plateau energy. The maximum impact parameter that can reduce the dissociation probability will therefore decrease from r_c to a lower value. Within the hard-hemisphere model, it is straightforward to estimate the importance of this "plateau effect". For initial energy E_i and plateau threshold E_p, the revised upper bound is $r_c' = r_c[(1+\sqrt{(E_p/E_i)})/2]^{1/2}$. With E_p=0.3 eV and E_i=0.5 eV, r_c'=0.942r_c. The plateau effect is therefore small, and cannot explain the fall in the observed blocking radius at high energies.

We conclude that a CO-induced activation barrier for surface dissociation must exist in the immediate vicinity of the adsorbed molecules, and extends somewhat beyond the hard-shell radius r_c of CO. Such an activation barrier would be encountered by D_2 molecules that strike a CO molecule but are not deflected through large scattering angles, and also by molecules that just miss a CO molecule. Hence, for D_2 molecules with incoming energy less than the activation barrier, the observed blocking cross sections would be expected to be somewhat larger than r_c. This behaviour is consistent with our experimental observations for E_i<0.35 eV.

At higher energies (>0.35 eV) the observed values of the blocking radius r_s decrease toward r_{eff} determined from the hard-hemisphere model. Molecules with this much incoming energy are apparently able to surmount the CO-induced activation barrier. A D_2 molecule that hits the surface near a CO molecule, or which hits a CO molecule but does not lose enough energy perpendicular to the surface to fall below the barrier, can now react. In the limit of incoming energy high above the CO-induced

barrier, we would expect the blocking radius to approach r_{eff}. The relatively sharp fall in r_s is consistent with the behaviour expected for an activated sticking process. Additional evidence for the existence of a CO-induced activation barrier is present in the data for the surfaces with higher θ_{CO}.

For θ_{CO} above the lattice-gas region (θ_{CO}>0.2 ML), it becomes necessary to consider the possible influence of collisions of an incoming D_2 molecule with more than one CO molecule. The CO overlayer leads to a more laterally corrugated potential-energy surface, and the CO-covered surface has fewer available sites for D_2 dissociation. Multiple collisions between D_2 and several CO molecules would reduce the apparent kinetic energy dependence of the D_2 dissociation probability compared with the bare Ru(0001) surface. If indirect, trapping-mediated dissociation represents a significant path on the high θ_{CO} surface, this mechanism should be most effective at low incident energies. As a result, S would increase with decreasing E_i. However, such a trend is not observed for high values of θ_{CO}. Instead, at high coverage, S increases only once E_i exceeds about 0.35 eV (see figure 4.1(a)). This behaviour is consistent with the molecule having to surmount an activation barrier. Since in this coverage region very little of the surface can be considered to be truly "CO-free", essentially all D_2 molecules will encounter the CO-induced barrier. In the low CO coverage region the barrier effectively increases the CO blocking cross section below 0.35 eV, whereas in the high CO coverage region it must be overcome for every D_2 dissociation.

Previously a cross section similar to our Σ_{CO} was reported by Michelsen and Luntz for D_2 dissociation on Pt(111) with chemisorbed O_2 (note that they modelled the influence of O_2 on the basis of the number of sites blocked per adsorbate) [56]. They concluded that O_2 mainly poisons D_2 dissociation sterically, because electronic effects arising as a result of O_2-induced changes in work function are small. In contrast, for H_2 dissociation on O-chemisorbed Ni(111) and Pt(111) [57, 58], O acts not only to poison sterically but also to promote H_2 dissociation. In the present study, steric hindrance by CO of D_2 dissociation is also proposed. However, in order to explain the rapid shrinking of the CO blocking area at low θ_{CO} for high E_i and the emergence of a relatively high dissociation probability for high kinetic energy D_2 at high θ_{CO}, we suggest that D_2 molecules that dissociate in the vicinity of adsorbed CO molecules must overcome a CO-induced activation barrier. This is not on the same length scale as the K-induced, long-range electronic modification that has been reported for D_2 dissociation on the K/Pt(111) surface [59]. For CO, only perturbation of the local surface electronic structure occurs.

4.5 Conclusions

We have measured the dissociation probability of D_2 on CO-covered Ru(0001) as a function of D_2 kinetic energy and CO coverage. We find that D_2 dissociation on this surface is an activated process. The effective CO cross section depends on the kinetic energy of D_2 at low CO coverage. At high coverage, D_2 dissociation occurs only for

relatively high kinetic energies. These results suggest that a CO-induced barrier for D_2 dissociation exists in the vicinity of CO molecules. At high CO coverage all D_2 dissociations occur via penetration of this CO-induced barrier.

Bibliography

[1] R.D. Kelley, D.W. Goodman, The Chemical Physics of Solid Surfaces and Heterogeneous Catalysis, Elsevier, New York, 1982.
[2] A.W. Kleyn, Chemical Society Reviews, **32** (2003) 87-95.
[3] G.A. Somorjai, Introduction to Surface Chemistry and Catalysis, Wiley, New York, 1994.
[4] J.M. White, S. Akhter, CRC Critical Reviews in Solid State and Materials Sciences, **14** (1988) 131-173.
[5] M.P. Kiskinova, Poisoning and Promotion in Catalysis Based on Surface Science Concepts and Experiments, Elsevier, Amsterdam, 1992.
[6] M. Johansson, O. Lytken, I. Chorkendorff, Surface Science, **602** (2008) 1863-1870.
[7] H.H. Storch, N. Golumbic, R.B. Anderson, The Fischer-Tropsch and Related Syntheses, John Whiley & Sons, Inc., New York, 1951.
[8] M.A. Vannice, Journal of Catalysis, **50** (1977) 228-236.
[9] P. Winslow, A.T. Bell, Journal of Catalysis, **94** (1985) 385-399.
[10] S. Kneitz, J. Gemeinhardt, H.-P. Steinrück, Surface Science, **440** (1999) 307-320.
[11] H. Pfnür, D. Menzel, The Journal of Chemical Physics, **79** (1983) 2400-2410.
[12] B. Riedmüller, I.M. Ciobîca, D.C. Papageorgopoulos, B. Berenbak, R.A. van Santen, A.W. Kleyn, Surface Science, **465** (2000) 347-360.
[13] B. Riedmüller, I.M. Ciobîca, D.C. Papageorgopoulos, F. Frechard, B. Berenbak, A.W. Kleyn, R.A. van Santen, The Journal of Chemical Physics, **115** (2001) 5244-5251.
[14] G. Blyholder, The Journal of Physical Chemistry, **68** (1964) 2772-2777.
[15] C. Stampfl, M. Scheffler, Physical Review B, **65** (2002) 155417.
[16] T.E. Madey, Surface Science, **79** (1979) 575-588.
[17] H. Pfnür, D. Menzel, F.M. Hoffmann, A. Ortega, A.M. Bradshaw, Surface Science, **93** (1980) 431-452.
[18] G.E. Thomas, W.H. Weinberg, The Journal of Chemical Physics, **70** (1979) 1437-1439
[19] M. Gierer, H. Bludau, H. Over, G. Ertl, Surface Science, **346** (1996) 64-72.
[20] G. Michalk, W. Moritz, H. Pfnür, D. Menzel, Surface Science, **129** (1983) 92-106.
[21] H. Over, M. Gierer, H. Bludau, G. Ertl, Physical Review B, **52** (1995) 16812-16829.
[22] H. Over, W. Moritz, G. Ertl, Physical Review Letters, **70** (1993) 315-318.
[23] H. Pfnür, D. Menzel, Surface Science, **148** (1984) 411-438
[24] J. Braun, K.L. Kostov, G. Witte, C. Wöll, The Journal of Chemical Physics, **106** (1997) 8262-8273.
[25] T. Kondo, H.S. Kato, M. Bonn, M. Kawai, The Journal of Chemical Physics, **127** (2007) 094703.
[26] P. Feulner, D. Menzel, Surface Science, **154** (1985) 465-488.
[27] I.M.N. Groot, H. Ueta, M.J.T.C. van der Niet, A.W. Kleyn, L.B.F. Juurlink, The Journal of Chemical Physics, **127** (2007) 244701.

[28] M. Lindroos, H. Pfnür, P. Feulner, D. Menzel, Surface Science, **180** (1987) 237-251.
[29] Y.-K. Sun, W.H. Weinberg, Surface Science, **214** (1989) L246-L252.
[30] D.E. Peebles, J.A. Schreifels, J.M. White, Surface Science, **116** (1982) 117-134.
[31] C.H. Mak, A.A. Deckert, S.M. George, The Journal of Chemical Physics, **89** (1988) 5242-5250.
[32] R.L.C. Wang, H.J. Kreuzer, P. Jakob, D. Menzel, The Journal of Chemical Physics, **111** (1999) 2115-2122
[33] B. Riedmüller, D.C. Papageorgopoulos, B. Berenbak, R.A. van Santen, A.W. Kleyn, Surface Science, **515** (2002) 323-336.
[34] B. Riedmüller, F. Giskes, D.G. van Loon, P. Lassing, A.W. Kleyn, Measurement Science & Technology, **13** (2002) 141-149.
[35] K. Kern, R. David, G. Comsa, The Journal of Chemical Physics, **82** (1985) 5673-5676.
[36] J.E. Pollard, D.J. Trevor, Y.T. Lee, D.A. Shirley, The Journal of Chemical Physics, **77** (1982) 4818-4825.
[37] D.A. King, M.G. Wells, Surface Science, **29** (1972) 454-482.
[38] D.A. King, M.G. Wells, Proceedings of the Royal Society London A, **339** (1974) 245-269.
[39] J.-S. McEwen, A. Eichler, The Journal of Chemical Physics, **126** (2007) 094701.
[40] S.H. Payne, J.-S. McEwen, H.J. Kreuzer, D. Menzel, Surface Science, **594** (2005) 240-262
[41] H. Pfnür, H.J. Heier, Berichte der Bunsen-Gesellschaft. Physical Chemistry, **90** (1986) 272-277.
[42] J.D. Beckerle, A.D. Johnson, Q.Y. Yang, S.T. Ceyer, The Journal of Chemical Physics, **91** (1989) 5756-5777.
[43] I.M. Ciobîca, A.W. Kleyn, R.A. van Santen, The Journal of Physical Chemistry B, **107** (2003) 164-172.
[44] A.A. Deckert, J.L. Brand, M.V. Arena, S.M. George, Surface Science, **208** (1989) 441-462.
[45] E.D. Williams, W.H. Weinberg, A.C. Sobrero, The Journal of Chemical Physics, **76** (1982) 1150-1161.
[46] E.D. Williams, W.H. Weinberg, Surface Science, **82** (1979) 93-101.
[47] B. Poelsema, G. Comsa, Scattering of Thermal Energy Atoms from Disordered Surfaces, Springer-Verlag, Berlin, 1989.
[48] H. Jónsson, J.H. Weare, A.C. Levi, Physical Review B, **30** (1984) 2241-2244
[49] B. Poelsema, G. Comsa, Faraday Discussions, **80** (1985) 247-256.
[50] B. Poelsema, S.T. de Zwart, G. Comsa, Physical Review Letters, **49** (1982) 578-581.
[51] B. Poelsema, S.T. de Zwart, G. Comsa, Physical Review Letters, **51** (1983) 522-522.
[52] H.P. Butz, R. Feltgen, H. Pauly, H. Vehmeyer, Zeitschrift für Physik, **247** (1971) 70-83.
[53] B.H. Choi, K.T. Tang, J.P. Toennies, The Journal of Chemical Physics, **107** (1997) 9437-9446.
[54] B.H. Choi, K.T. Tang, J.P. Toennies, The Journal of Chemical Physics, **109** (1998) 6504-6504.
[55] P. Jankowski, K. Szalewicz, The Journal of Chemical Physics, **123** (2005) 104301.
[56] H.A. Michelsen, A.C. Luntz, Chemical Physics Letters, **187** (1991) 555-558.

[57] C. Resch, V. Zhukov, A. Lugstein, H.F. Berger, A. Winkler, K.D. Rendulic, Chemical Physics, **177** (1993) 421-431.
[58] L.K. Verheij, M.B. Hugenschmidt, Surface Science, **324** (1995) 185-201.
[59] J.K. Brown, A.C. Luntz, P.A. Schultz, The Journal of Chemical Physics, **95** (1991) 3767-3774.